doi:10.3969/j. issn. 1673-9736. 2017. 04. 07
Article ID: 1673-9736(2017)04-0246-07

Application of high-frequency magnetotelluric method in porphyry copper deposit exploration: a case study of Duobaoshan deposit area

LIU Caihua, QU Xin*, FENG Xuan, TIAN You, LIU Yang, QIAO Hanqing and WANG Shiyu

College of Geo-Exploration Science and Technology, Jilin University, Changchun 130026, China

Abstract: The Duobaoshan mine area in Heilongjiang is located in the northeast section of Xingmeng orogenic belt and is in the west side of Hegang Mountain-Heihe fault zone. There exist many deposits in this area, and its metallogenic conditions are superior, which has been one of the hotspots in geological prospecting and metallogenic research in Northeast China. On the basis of previous studies, the authors used the EH-4 electromagnetic imaging system to carry out the data acquisition of three survey lines in Woduhe Village, Duobaoshan Town, Nenjiang County. Through the analysis of apparent resistivity section under TE and TM polarization modes, integrating regional geological data, it is concluded that: ① the electrical characteristics of the metal ore in this area show a relatively low resistance, and according to its resistivity difference with surrounding rocks, the geometrical structures and apparent resistivity parameters of the low resistivity bodies in the lower section of the survey line are defined, and the electrical anomalies can be identified; ②faults F1 and F2 may have a good metallogenic environment, so they are recommended for further exploration; ③ low resistance metal ore bodies have good correlation with local small structures or faults, which may play an iconic role for the delineation of key target areas; ④ in the process of using apparent resistivity to define the geometric structures of ore bodies underground, comprehensive analysis integrating the advantages of TE and TM models should be carry out to achieve more reliable inversion results.

Key words: magnetotelluric Sounding (MT); apparent resistivity; Xing'an Mongolia orogenic belt; porphyry copper deposit; Duobaoshan ore concentration area

0 Introduction

Porphyry copper deposits are currently the largest source of copper ore and the dominant source of copper formed by hydrothermal processes associated with magmatism (Hou *et al*., 2007). Thus, detection and exploration of porphyry copper deposits has great economic significance. The Duobaoshan porphyry Cu-Mo-(Au) deposit is one of the largest Cu (Mo) deposits in the Central Asian orogenic belt and contains proven reserves of 3.35×10^6 tons of Cu, 73 tons of Au, 0.15×10^6 tons of Mo, and 1 046 tons of Ag, with average grades of 0.52% for Cu, 0.02% for Mo, 0.16–0.35 g/t for Au and 4.5–7.7 g/t for Ag. The deposit is located in Nenjiang County of Heilongjiang Province and situated to the northeast of Xing'an-Mon-

Received 5 May 2017, accepted 28 May 2017
* Corresponding author (E-mail: quxin1987@jlu.edu.cn)
Supported by National Key Basic Research Program of China (973 Program) (No. 3B813C254423).

golian orogenic belt, in the west side of the boundary fault (Hegenshan-Heihe fault) between Songnen block and Xing'an block. Many hydrothermal veins and porphyry Cu (Mo) deposits, such as the Tongshan, Xiaoduobaoshan, Jiguanshan, Yuejin and Xiaogushan, have been discovered near the Duobaoshan deposit area. The geological, geochemical and geophysical features of the Duobaoshan deposit area have been studied since its discovery (Hao *et al* (Hao, 2015; Zhao *et al*., 2011; Liu *et al*., 2008; Zhao *et al*., 2011; Wang *et al.*, 2008; Du, 2012; Chen *et al*., 2012; Du *et al*., 1988; Gong *et al*., 2013; Zeng *et al*., 2014; Zhao *et al*., 1995) (Fig. 1). Based on the previous works, we collected geophysical data in this area and processed the electromagnetic data for further study.

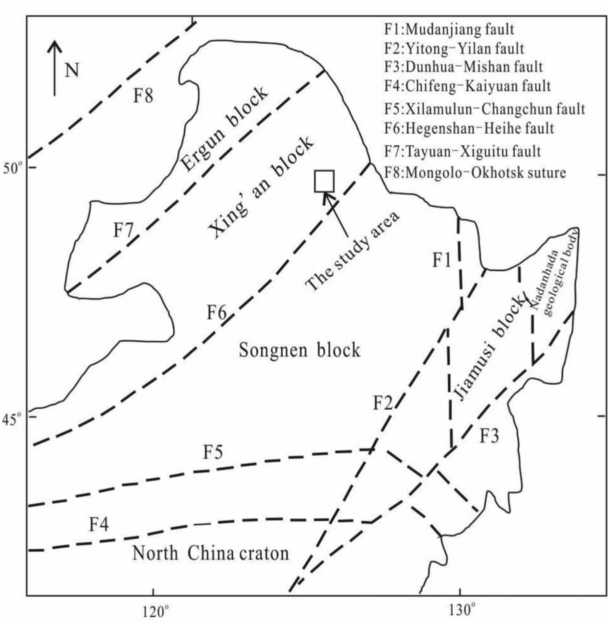

Fig. 1 Sketch map of tectonic location of Duobaoshan ore concentration area (Hao, 2015)

1 Profile survey and parameters of continuous conductivity of EH4

Magnetotelluric Sounding (MT) is a geophysical method that uses natural electromagnetic fields as field sources to study the internal electrical characteristics of the Earth (Tikhonov, 1950; Cagniard, 1953; Chave, 2012; Simpson, 2005; Liu *et al.*, 2012). Currently, well-known MT instruments include: the V-series (V5-2000 or V8) of Phoenix in Canada; the GMS-series (GMS-06 or GMS-07) of Metronix in Germany; the GDP-series (GDP-16 or GDP-32) of Zonge in America and the EH-4 jointly produced by Geotronics and EMI in America. EH-4 is a frequency and electromagnetic observation system that can use both natural electromagnetic field sources and artificial field sources (Liu *et al*., 2012). The measurement band is between 10Hz - 100KHz which can observe electric changes and obtain information to the depth of 1 000 m from the Earth's surface. By analyzing electric information it can successfully resolve geological problems, in engineering geological investigation, environmental monitoring, and underground water research as well as mineral and geothermal exploration. This system can be used under different geological conditions especially in bad field environment (Liu *et al*., 2012).

If natural electromagnetic fields enter each isotropic layered stratum evenly and perpendicularly in the form of plane waves, the impedance frequency characteristics were transformed into a form of apparent resistivity (Cargniard, 1953):

$$\rho_s = \frac{|Z|^2}{5f} \tag{1}$$

Where ρ_s is apparent resistivity, f is frequency, Z is wave impendence. It is defined as follows:

$$|Z| = \frac{|E_x|}{|H_y|} = \frac{|E_y|}{|H_x|} \tag{2}$$

Where E_x is the horizontal component of the electrical field in the x direction; E_y is the vertical component of the electrical field in the y direction; H_x is the horizontal component of the magnetic field in the x direction; H_y is the vertical component of the electrical field in the y direction.

In the studied area, distance between the two survey points is 50 m. There are three survey lines: L1 from 125.76°E, 50.44°N to 125.75°E, 50.46°N, L2 from 125.75°E,50.46°N to 125.80°E, 50.44°N, L3 from 125.94°E, 50.42°N, to 125.86°E, 50.42°N, respectively. The total number of physical survey points is 231. We applied MTSoft2D to preprocess the data, eliminate the incorrect values, carry out static correction, and perform spatial filtering. Then we can obtain the pseudo section of the apparent resistivity, as shown in Figs. 2–4 (both frequency and apparent resistivity are taken logarithm value).

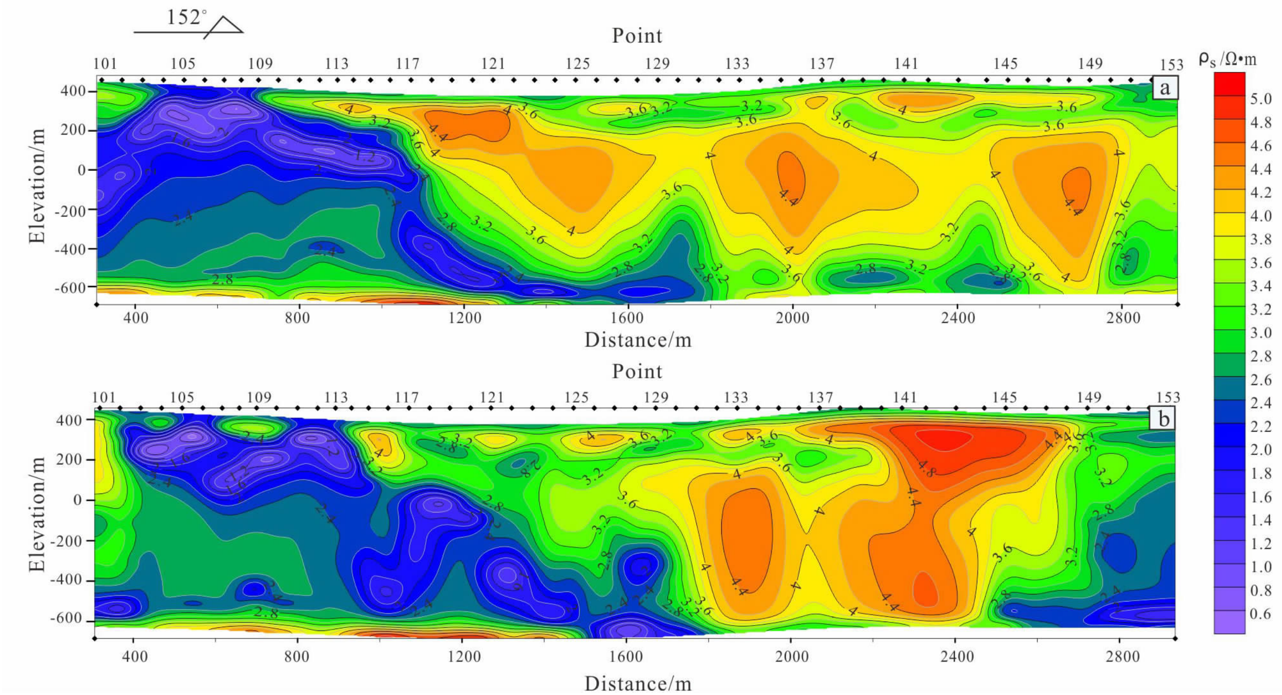

Fig. 2 Comparison between TE (a) and TM (b) mode in L1 profile

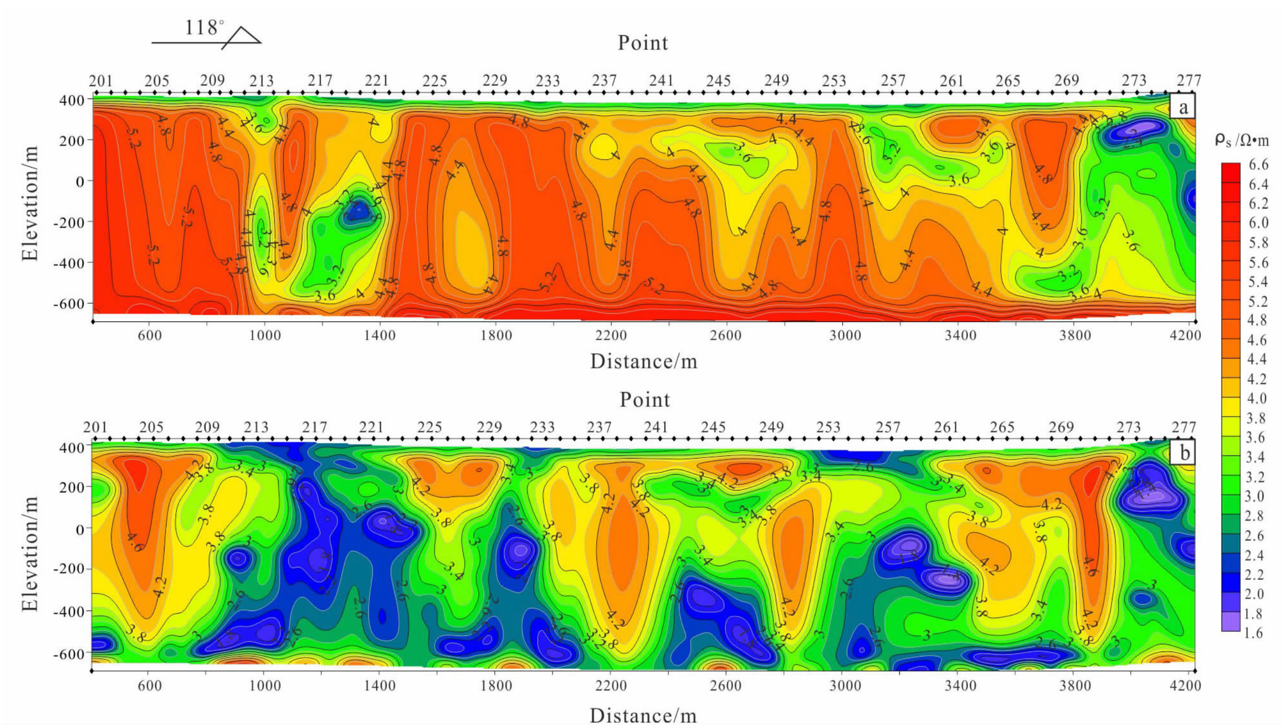

Fig. 3 Comparison between TE (a) and TM (b) mode in L2 profile

2 Data inversion

In MT, TE polarization mode and TM polarization mode have different advantages in reflecting the trend of geological bodies. For general survey lines which are perpendicular to the geological body, TM has a better horizontal resolution and the TE has a better vertical resolution. First, we used the result of the 2-dimensional Bostick transform as the initial model. Then we used the inversion result of the 1-dimensional Occam inversion as the initial model to make a 2-dimensional Occam inversion. During the inversion process, the apparent resistivity and phase curves were rotated to be perpendicular to the direction of the survey lines under TE polarization mode and parallel to the direction of the survey lines under TM polarization mode. In order to overcome the inherent limitations in these modes, and take the advantages of TE and TM polarization modes, we made single inversion on TE and TM respectively and a joint inversion of both TE and TM polarization modes. Figs. 2–4 show the apparent resistivity ratios of the TE and TM polarization modes of the lines L1, L2 and L3, respectively. Generally speaking, the TE mode and TM mode are obviously different in their spatial form of high and low resistivity, however, they are similar in general distribution trends. In the figures of TM mode, there are low-resistance responses at the horizontal location of the metallic mineral lens in the geological map, while the response given by the TE mode is insignificant. This indicates that the resistivity of metallic mineral lens is not much lower than the surrounding rocks, and the scale of the metallic mineral lens is not very large, which does not result in an anomaly in the TM mode.

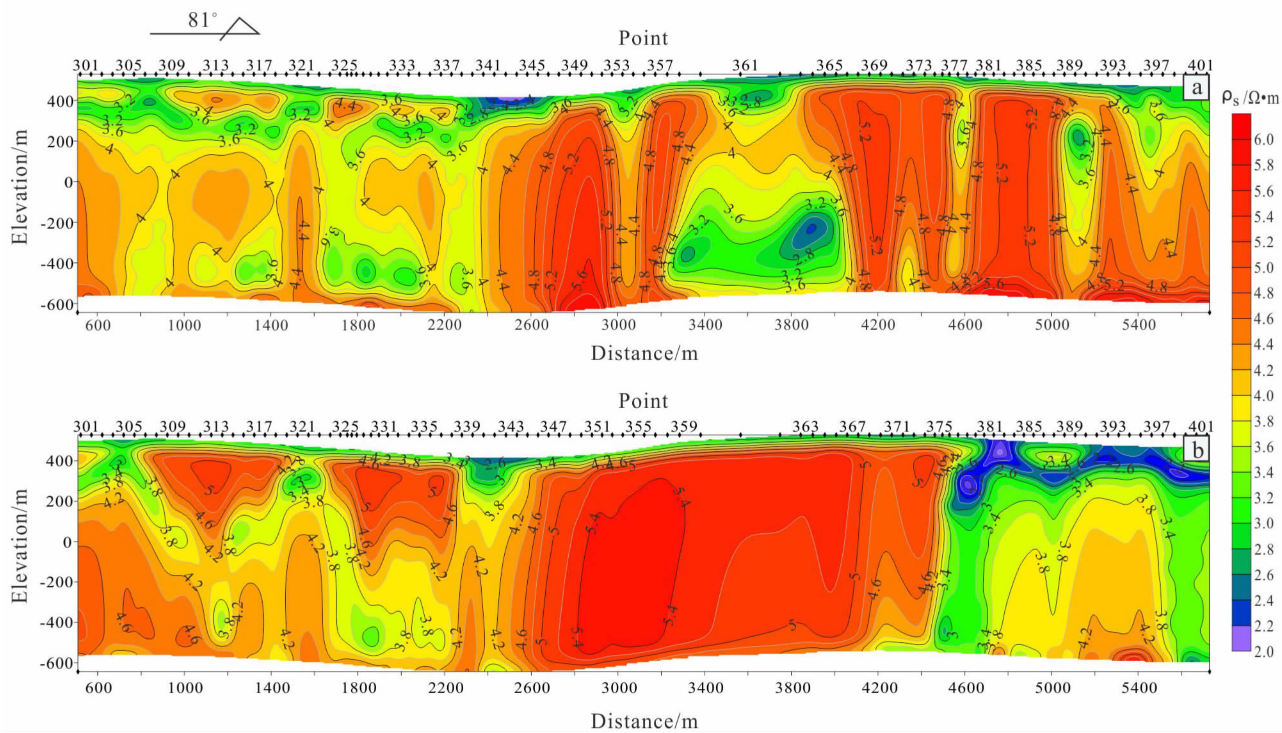

Fig. 4 Comparison between TE (a) and TM (b) mode in L3 profile

3 Geological interpretation

Fig. 5 is a section view of resistivity inversion of L1 line. According to rock electrical statistics of Gong (2013), the resistivity of the profile is higher on the whole. In the vertical direction, Quaternary sedimentary layer and andesite in Duobaoshan Formation thickened gradually from the south to the north, whose distribution range is 100 – 200 m. In the horizontal direction, from points 101 to 112, the resistivity changes greatly. Between points 102 to 111, there is a narrow metamorphic siltstone low resistivity body, and the resistivity on the right side is higher. There is a fault at point 112, and the narrow and low resistivity body may be intrusive veins along the fault. From points 112 to 148, the resistivity increases with depth gradually. At about 100 m below the ground level, the isoclines are denser and the resistivity changes greatly. This may correspond to the boundary between two geological bodies. The upper half of the area is a metamorphic siltstone block with relatively low resistance of about 1 000 Ω · m, whereas the lower half of this area is estimated as a high resistance block of andesite and andesitic porphyrite, with little variation in resistance. From points 148 to 153, the resistivity diagram shows a low resistivity less than 1 000 Ω · m.

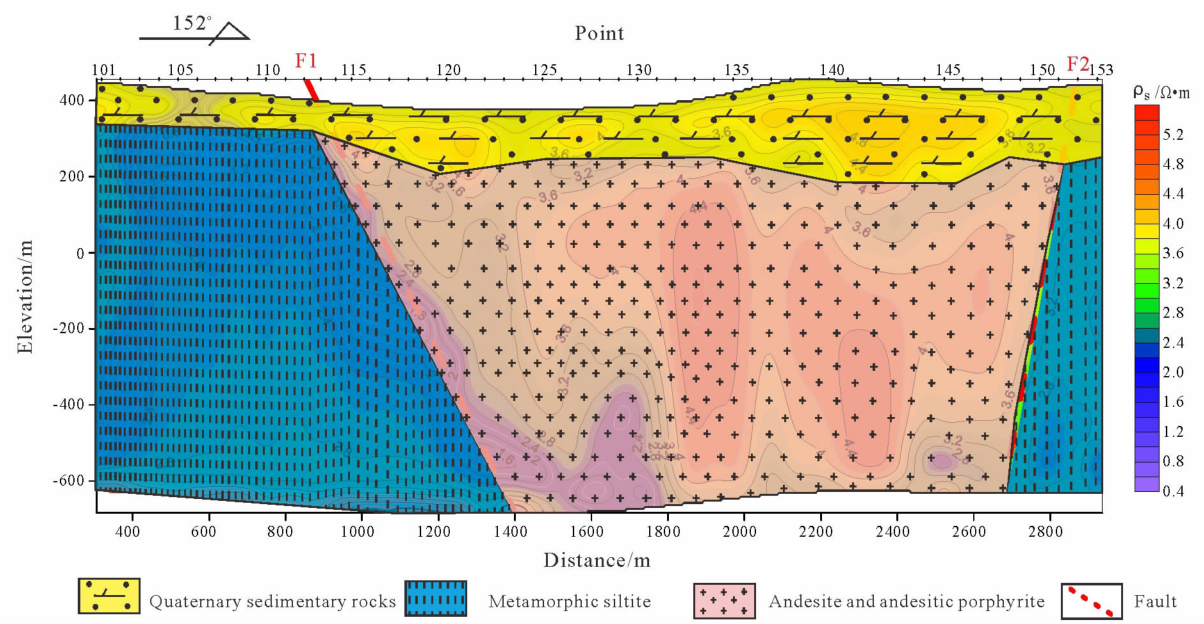

Fig. 5 Joint inversion of TE and TM mode and geological interpretation on L1 profile

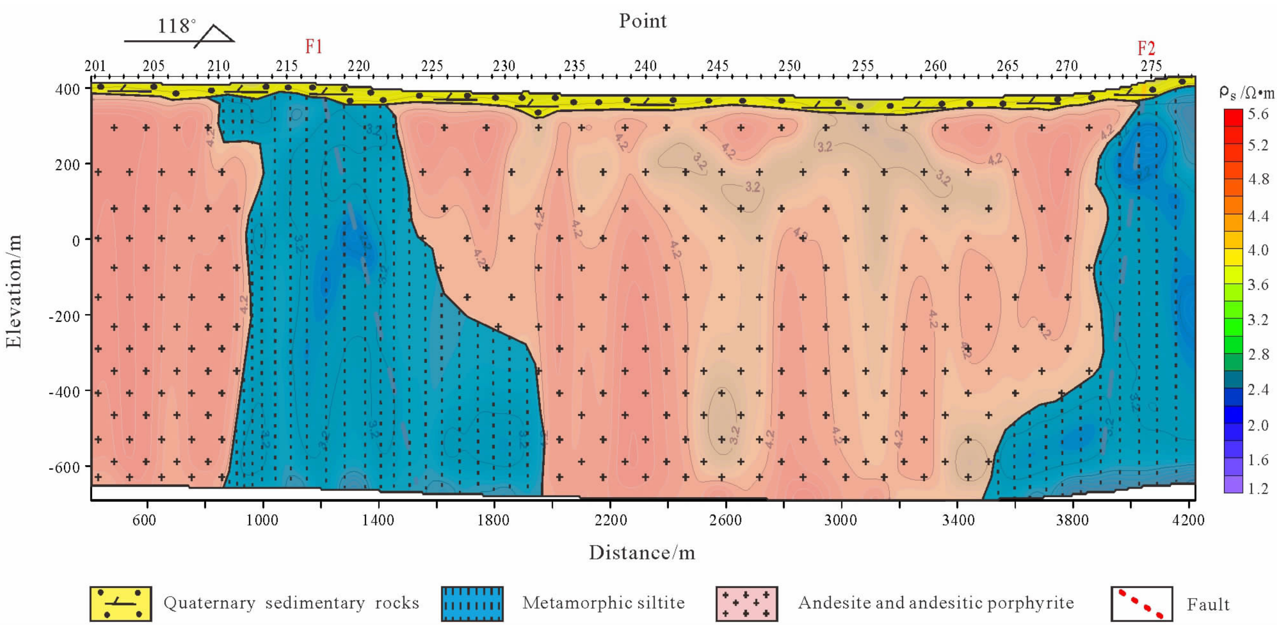

Fig. 6 Joint inversion of TE and TM mode and geological interpretation on L2 profile

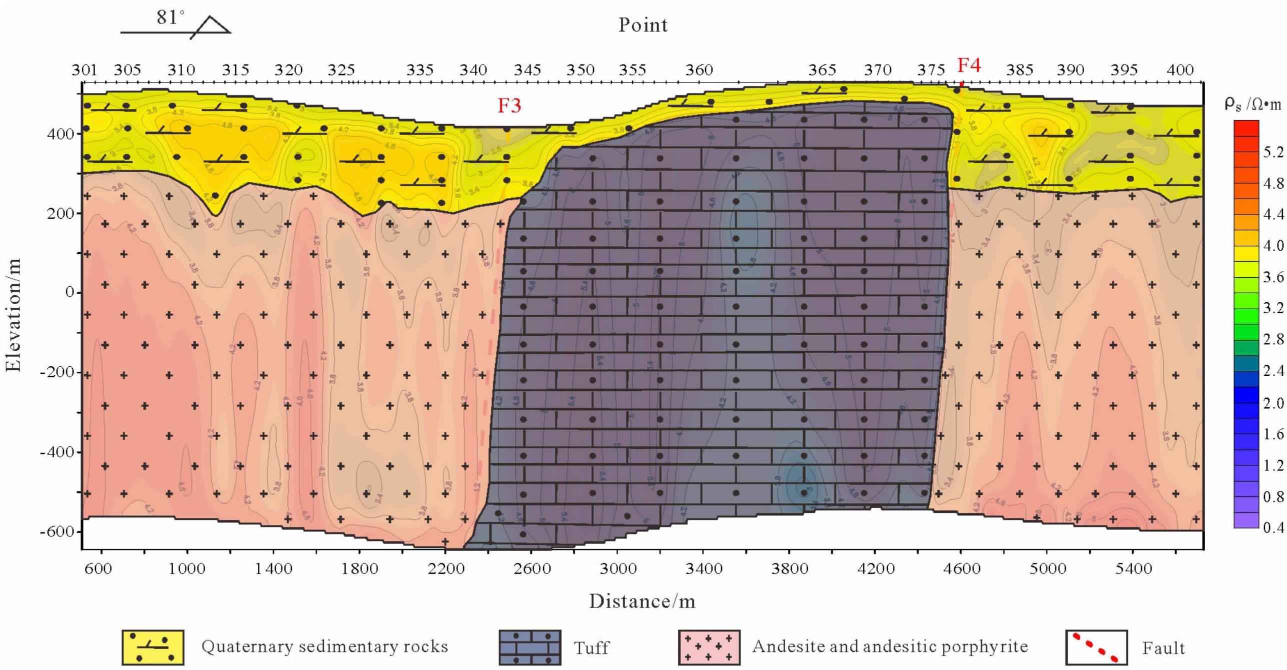

Fig. 7 Joint inversion of TE and TM mode and geological interpretation on L3 profile

The resistivity of this section changes slowly and the low resistivity metamorphic siltstone extends from the surface to the deep, with some local minor resistivity anomalies.

Fig. 6 is the L2 resistivity inversion profile. The length of this line is 3 850 m. The resistivity profile of this line shows significant variation. It is divided into three parts by two faults. At point 210 near the fault, both sides are high resistance andesite and andesitic porphyrite. The fault shows a relatively low resistance with certain width. At the left side of the fault, except the low resistance near surface, it shows high resistance from 100 m below ground surface downwards, with no obvious electrical variations. Thus we presume it is one geological body. In general, the resistivity between the two faults is relatively high, but the central part shows relatively low resistance with slow transition to the high resistance. The low resistivity region is divided into two blocks by the high resistance bodies from the lower part. In the right side of the fault at point 273 it shows continuous low resistivity overall, with only a small amount of high resistance at the bottom.

Fig. 7 is the L3 resistivity inversion profile. The length of the line is 5 200 m. From the resistivity profile, it is indicated that the overall resistance varies considerably. From the surface to the depth of 200 – 400 m, it consists of continuous low resistance Quaternary sediments with some metamorphic siltstone layers. The lower section underlying the Quaternary sediments and metamorphic siltstone is divided into three parts by two faults, i. e. fault F3 at point 343 and fault F4 at point 379. The resistivity of the first part increases in the vertical direction with depth, showing variation in resistance, and it is inferred as Andesite. It is speculated that the high resistance body in the right side of fault F3 is tuff. In the right side of fault F4 at point 379, from the ground down to 600 m it consists of discontinuous low resistance layers, which is similar to the left side of F3 and is therefore inferred to be andesite.

4 conclusions

(1) The electrical characteristics of the metal ore in this area show a relatively low resistance, and according to its resistivity difference with surrounding

rocks, the geometrical structures and apparent resistivity parameters of the low resistivity bodies in the lower part of the survey line are determined, and the electrical anomalies can be identified.

(2) Faults F1 and F2 indicate a favorable metallogenic environment, which suggests for the further exploration.

(3) Low resistance metal ore bodies have good correlation with local small structures or faults, which may play an iconic role for the delineation of key target areas.

(4) In the process of using visual resistivity identify the geometric structure of ore bodies underground, comprehensive analysis integrating the advantages of TE and TM models should be carried out to obtain more reliable inversion results.

References

Cagniard L. 1953. Basic theory of the Magneto-telluric method of Geophysical prospecting. *Geophysics*, **18** (3): 605-635.

Chave A D, Jones A G. 2012. The magnetotelluric method: theory and practice. Cambridge: Cambridge University Press, 1-7.

Chen Y J, Zhang C, Li N, *et al.* 2012. Geology of the Mo deposits in northeast China. *Journal of Jilin University: Earth Science Edition*, **42**(5): 1223-1268. (in Chinese with English abstract)

Du Qi. 1998. Duobaoshan porphyry copper deposits. Beijing: Geological Publishing House, 282-310.

Du Y J. 2012. The metallogenic characteristics and prospecting direction of Duobaoshan Cu-Au metallogenic belt, Heilongjiang province: master's degree thesis. Changchun: Jilin University.

Gong S P, Ding W Z, Wang M M, *et al.* 2013. The application effect of phase-IP method in Duobaoshan perspective survey. *Computing Techniques for Geophysical and Geochemical Exploration*, **35**(5): 524-529. (in Chinese with English abstract)

Hao Y J. 2015. Mineralization and metallogenic regularity of Duobaoshan ore concentration area in Heilongjiang province, Northeast China: PhD thesis. Changchun: Jilin University.

Hou Z Q, Pan X F, Yang Z M, *et al.* 2007. Porphyry Cu-(Mo-Au) deposits no related to oceanic-slab subduction: examples from Chinese porphyry deposits in continental settings. *Geoscience*, **21**(2): 332-351. (in Chinese with English abstract)

Liu J X, Tong X Z, Guo R W, *et al.* 2012. Magnetotelluric exploration. Beijing: Science Press, 185-190.

Liu Y, Cheng X Z, Wang X C, *et al.* 2008. Cu-source and enrichment laws of the Duobaoshan porphyry copper deposit in Heilongjiang province. *Chinese Journal of Geology*, **43**(4): 671-684. (in Chinese with English abstract)

Simpson F, Bahr K. 2005. Practical magnetotellurics. Cambridge: Cambridge University Press, 1-5.

Tan C Y, Wang G H, Li Y S. 2010. New progress and significance on the mineral exploration in Duobaoshan mineralization area, Heilongjiang, China. *Geological Bulletin of China*, **29**(2/3): 436-445. (in Chinese with English abstract)

Tikhonov A N. 1950. On determining electrical characteristics of the deep layers of the Earth's crust. *Doklady*, **73**(2): 295-297.

Wang H Y, Ma L L, Wang Z. 2008. Geological character and genesis of Sankuanggou copper (iron) mineral deposit, Duobaoshan area, Heilongjiang Province. *Journal of Jilin University: Earth Science Edition*, **38**(Suppl.): 214-218. (in Chinese with English abstract)

Zeng H, Zhao Y Y, Fu J J, *et al.* 2014. The characters both sulfur isotope and peripheral geochemical anomalies in Duobaoshan deposit//Annual Meeting of Chinese Geoscience Union(CGU). (in Chinese with English abstract)

Zhao Y Y, Wang J P, Zhao G J, *et al.* 2011. Metallogenic regularity and prospecting direction of Duobaoshan ore field, Heilongjiang province, China. *Journal of Jilin University: Earth Science Edition*, **41**(6): 1676-1688. (in Chinese with English abstract)

Zhao Y Y, Zhao G J. 1995. Geochemical characteristic of the Duobaoshan copper orefieldree and its genetic model in Heilongjiang province. *Jilin Geology*, **14**(2): 71-78. (in Chinese with English abstract)

Zhao Z H, Zheng W Z, Qu H, *et al.* 2012. Cu-Au mineralization and metallogenic regularity of Duobaoshan area, Heilongjiang Province. *Mineral Deposits*, **31**(3): 601-614. (in Chinese with English abstract)